Effects of the size and matrix microstructure on compression of borosilicate spheres -Zn22Al2Cu composites with foam behaviour

R.C. Flores-Marquez[a], J.A. Aragon-Lezama[b] and G. Torres Villaseñor[b]

[a]*Área de Ciencia de Materiales, Departamento de Materiales, Universidad Autónoma Metropolitana-A*
Avenida San Pablo 180, Colonia Reynosa Tamaulipas, 02200, CDMX, México.
[b]*Departamento de Metálicos y Cerámicos, Instituto de Investigaciones en Materiales,*
Universidad Nacional Autónoma de México, Apartado Postal 70-360, CDMX, México,
Tel: (55) 5318-9475 Ext. 9475   Fax (55) 53823998
e-mail: alja@correo.azc.uam.mx

Borosilicate spheres - Zn22Al2Cu composites with a 2.9 g/cm^3 density were prepared to assess whether changes in size affect the compression behaviour, and whether this effect depends on the alloy matrix microstructure. The composite material was manufactured first by alloy melting, then by sphere submersion into the liquid alloy, and finally by air-cooling the resulting mixture to room temperature. The matrix microstructures used separately were as-cast microstructure and fine microstructure. They were characterized by optical and scanning electron microscopies as well as by an energy dispersive X-ray spectroscopy compositional analysis of polished and etched samples. The compression was tested in three samples of each size at a 1 mm/min crosshead speed. The compression curves of composites with fine microstructure in matrix are similar in shape to those of ideal metallic foams, whereas curves of the composites having as-cast microstructure in matrix have a shape like compression curves of Zn and Al$_2$O$_3$ foams. The as-cast microstructure is more susceptible to changes in size than is the fine microstructure. Thus, the foam compression behaviour of borosilicate spheres - Zn22Al2Cu composites changes with the increase in size, and this change depends on the matrix microstructure.

Keywords: Zn22Al2Cu composite; foam behaviour; compression; change in size; change in microstructure

El material compuesto de Zn22Al2Cu con esferas de borosilicato y densidad de 2.9 g/cm^3, fue elaborado para establecer si el cambio de sus dimensiones tiene efecto en su comportamiento ante la compresión, y si este efecto es distinto según la microestructura en la aleación matriz. El material se manufacturó fundiendo primero la aleación, sumergiendo después las esferas en ésta y enfriando paulatinamente la mezcla resultante al aire. Las microestructuras en la matriz fueron por separado de colada y fina. Estas fueron caracterizadas con microscopio óptico y electrónico de barrido y análisis composicional por EDS, en muestras pulidas y atacadas químicamente. Se ensayó en compresión tres muestras de cada uno de tres tamaños diferentes a una velocidad de cabezal de 1 mm/min. La forma de la curva en compresión del material compuesto es cercana a la de espumas metálicas ideales, cuando la microestructura en la matriz es fina, y parecida a la de espumas de Zn o Al$_2$O$_3$, cuando la microestructura es de colada. La microestructura de colada es más susceptible al cambio de dimensiones que la microestructura fina. Luego, el comportamiento en compresión tipo espuma del material compuesto de Zn22Al2Cu con esferas de borosilicato, cambia al aumentar sus dimensiones y es distinto el cambio según la microestructura en su matriz.

Descriptores: Materiales compuestos de Zn22Al2Cu; comportamiento de espuma; compresión; cambio de dimensiones; cambio de microestructura

1. Introduction

Some of the key properties of the Zn22Al2Cu alloy are its corrosion resistance, which is higher than that of galvanised products, its ability to be laminated, to be superplastic under suitable conditions, and to be welded [1].

The Zn22Al2Cu alloy features a typical as-cast microstructure, consisting of dendrites and inter-dendritic regions, or a microstructure with very fine and alternating α and β phases, abundant in Al and Zn, respectively. This is achieved when tempering this alloy by heating to a temperature higher than 275°C (to become a β stable phase only) and cooling to approximately 0°C [2].

This alloy also presents a pearlite eutectoid microstructure consisting of alternating α and β phases with a lamellar shape when slowly cooled inside an oven from a temperature higher than 275°C to room temperature [3].

Because of the interesting properties of the Zn22Al2Cu alloy, it has been considered as a matrix for composites or cellular materials for structural purposes in several research studies.

For example, the Zn22Al2Cu - ZnO composite has already been prepared and characterized by powder metallurgy, using reactive grade powders of the elements. The results showed that increasing the ZnO amount delays the formation of the pearlite component and considerably reinforces the matrix [4].

In another study, composites of this alloy with structural components of hydroxyapatite, Al_2O_3 and graphite were separately prepared from mixtures of alloy powders with the aforementioned components, also by powder metallurgy, achieving different reinforcements [5].

On the other hand, metal matrix syntactic foams, MMSFs, and metal composite foams, MCFs, have been the research topics of growing interest in recent years [6-14]. A MMSF is a material having hollow spheres [15,16], and a MCF has a second phase with pores (cells or voids) or a second phase without pores and hollow spheres in matrix [17].

Several of these materials have been developed and studied using matrices of Al, a review article was written by [18]., Zn [19] or the base alloy of eutectoid composition Zn22Al [20,21]. MMSFs or MCFs with matrix Zn22Al2Cu have not yet been elaborated.

In a recent study [22], solid glass spheres - Zn22Al2Cu composites, with different densities and matrix microstructures (as - cast and fine) were prepared and characterized. The results showed that these composites behave similarly to foam under compression, albeit with substantially higher collapse (or yield) and plateau stresses than conventional foams. Even though, this material does not have hollow spheres or cells anywhere. That is, this material is not a MMSF nor MCF.

The present study assesses the effect of changes in the size of the solid borosilicate spheres - Zn22Al2Cu com-posite on its compression behaviour using two different microstructures in its matrix.

2. Experimental

2.1. Composite preparation

The raw materials for the preparation of the composites were 99.99% pure Zn, 99.97% pure Al, 99.999% pure electrolytic Cu and borosilicate spheres 4 mm in diameter, with a melting temperature of 1100°C and a density of 2.5 g/cm³. Further characteristics of the spheres and their chemical composition, how were provide by the seller Ornela Ltd., are presented in Table I.

TABLE I. Characteristics of glass spheres.

Chemical analysis	SiO2: 61-67%; Na2O: 10-18%;
	CaO: 5-10%; Al_2O_3: 3-8%;
	B_2O: 1-5% and MgO: 0.5-3%
Lead content	Contains no lead
Elastic modulus	78-85 GPa
Vickers microhardness	970 kp/cm²
Density	2.5 ± 0.04 g/cm³
Diameter	4.0 ± 0.3 mm

FIGURE 1. A face of borosilicate spheres - Zn22Al2Cu composite. M, matrix.

The composites were prepared melting Zn inside a crucible, previously coated with zirconia, in a muffle furnace at 700°C, subsequently incorporating Al and finally Cu. In another furnace, a crucible with the spheres had been preheated to 400°C. The spheres were added to the liquid alloy and were pushed with a piston to prevent flotation while the mixture was air-cooled. Figure 1 shows a face of the composite prepared and cut just in half.

2.2. Alloy matrix microstructures

The composites prepared were halved. One-half was subjected to no further treatment, maintaining the microstructure resulting from the composite preparation, the as-cast microstructure. The other half of material, was subjected to heat treatment, homogenisation and tempering, which consisted of heating the piece in a muffle furnace at a stable state to 350°C for 45.5 h and then quickly cooling the piece to 0°C in an ice bath to obtain a very fine micro-structure.

2.3. Metallographic Preparation

One side of the composite samples with the as-cast microstructure and one side of the composites with the fine matrix microstructure were prepared for metallographic studies: sanded with abrasive papers of different grit sizes, mirror-polished with 0.3 mm and 0.05 mm alumina, and separately suspended in ethyl alcohol. The surfaces were finally etched by submersion in ethyl alcohol with 1% HNO_3 for 3 s to reveal their microstructure.

The samples with the as-cast or very fine microstruc-ture were polished as mentioned above for observation under a scanning electron microscope (SEM), albeit with-out etch-

FIGURE 2. Samples of the three sizes used for the compression test.

TABLE II. Test sample sizes and number.

Base, mm^2	Height, mm	Sample number
8×8	16	3
10×10	20	3
12×12	24	3

ing. Subsequently, the samples were cleaned twice in acetone and then in an isopropyl alcohol ultra-sound bath.

Samples of both microstructures were observed, analyzed and photographed at different magnifications under an Olympus PMG3 Inverted Metallurgical Microscope fitted with an Olympus C 5050 camera. The surfaces of the samples prepared for SEM were observed, analyzed and imaged at three magnifications, using secondary and backscattering electrons signals. Then, the composition of each microstructure was analyzed by energy dispersive X-ray spectroscopy (EDS).

2.4. Compression tests

Three samples for compression tests were obtained of each one of the three different sizes (Table II and Fig. 2) using a silicon carbide grinding wheel. Dimensions of the three sizes followed a 2:1 relationship.

The density was determined by measuring all the sizes and masses of samples that would be used to assess the compression behaviour, and resulting data were used to assess the mean density of each size. The average of all mean densities was 2.9045 ± 0.2021 g/cm^3.

The compression tests were performed on a Universal Testing Machine, Instron 1125, using a 1 mm/min cross-head speed. The values of each test were processed and averaged to construct the stress-deformation curve for each sample size.

3. Results

3.1. Alloy matrix microstructures

The as-cast matrix microstructure is shown in a set of images in Fig. 3. This microstructure consists of grey dendrites and light inter-dendritic regions. The latter are an intercalated combination of light and dark lamellae, as shown in Fig. 3c. The dendrites feature a submicrostructure of very fine phases alternating between dark and light shades (Fig. 3e).

The results from the compositional analysis by EDS of the dendrites and inter-dendritic regions are presented in Table III.
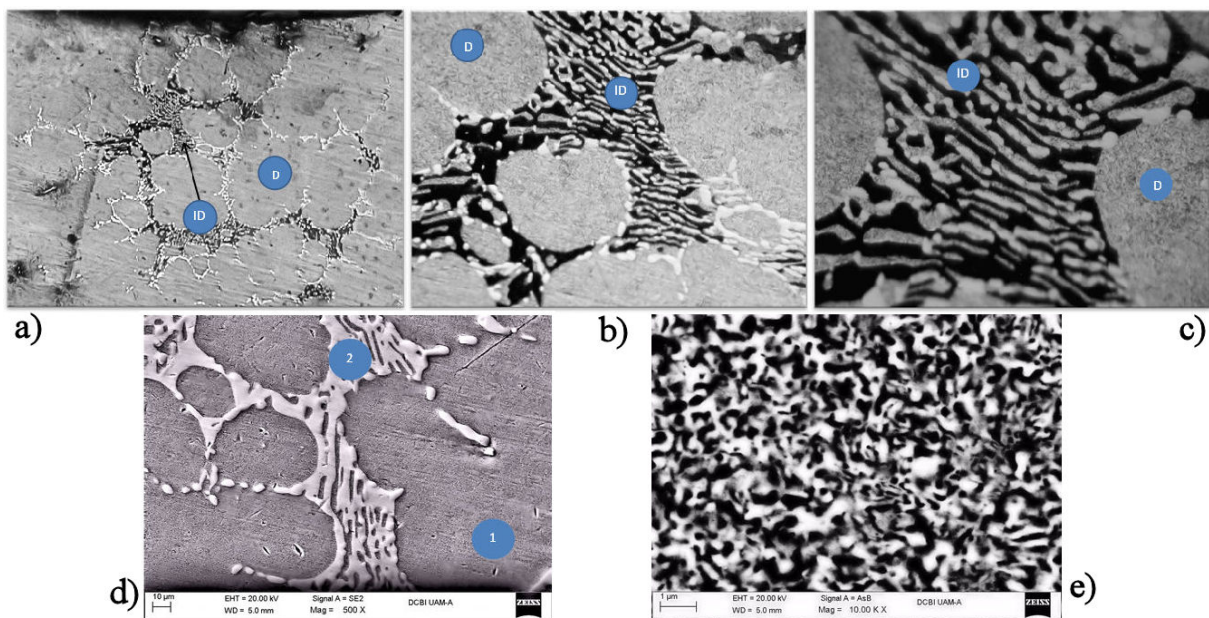
FIGURE 3. a) General view, 62X. b) Detail of Fig. 3a, 310X. c) Detail of Fig. 3b, 620X. d) General view. e) Dendrite sub-microstructure. As-cast matrix microstructure of the Zn22Al2Cu alloy: a), b) and c) under an optical microscope; d) and e) under an electron microscope. ID, inter-dendritic region; D, dendrite. Points 1 and 2 shown in d) were analyzed by EDS.
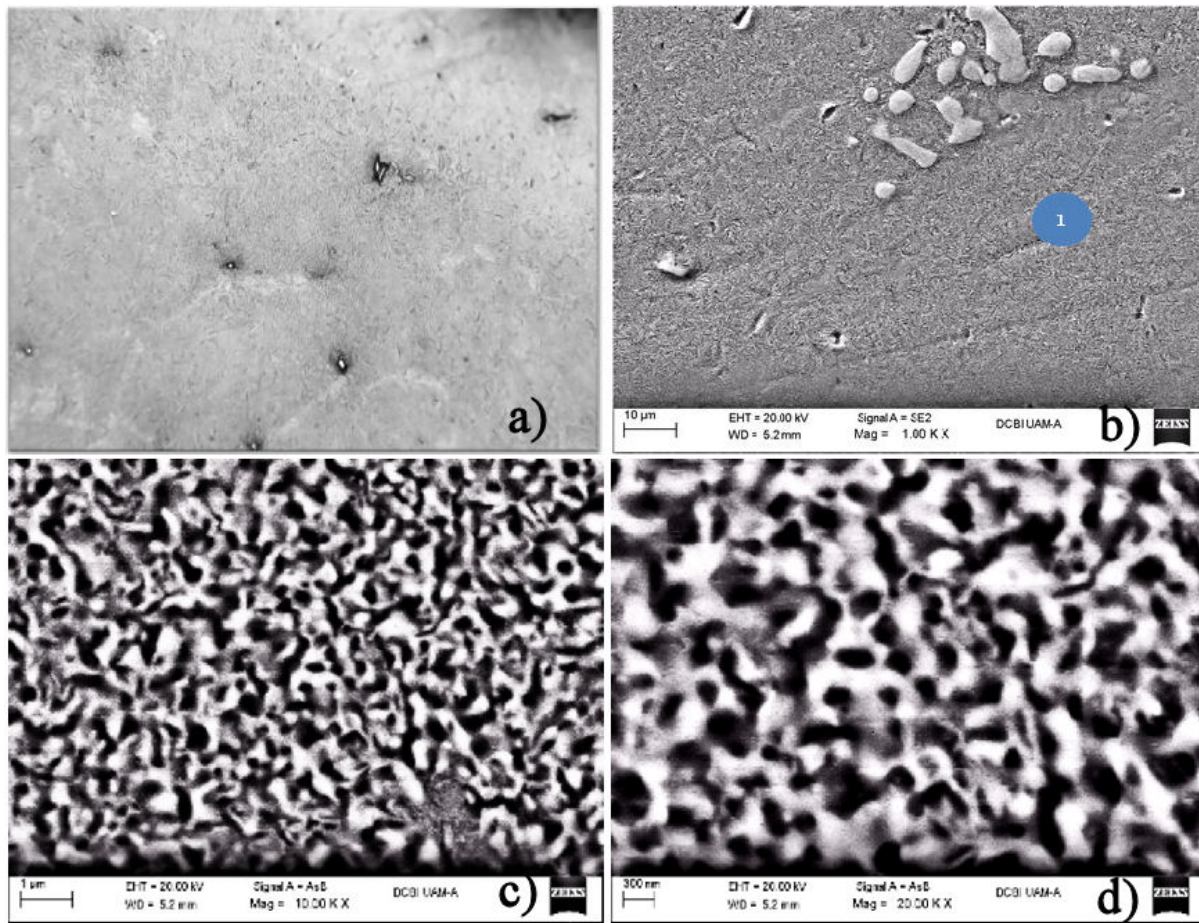
FIGURE 4. a) General view, 62X. b) General View. c) Detail of the grey area, marked with 1 in Fig. 4b. d) Detail of a zone of Fig. 4c. Microstructure obtained by thermal treatment, showing a smooth wide surface containing a substructure of fine and alternating constituents, with light and dark shades: a) optical microscope; b), c) and d) scanning electron microscope.

TABLE III. Composition of the components of the as-cast matrix microstructure, as determined by EDS.

Constituent	Element (% weight)			Analysis site (see Fig. 3d)
Dendrite	Zn	Al	Cu	
	77.77	20.88	1.35	Point 1
Inter-dendritic region	94.73	2.02	3.25	Point 2

TABLE IV. Composition of the grey, wide and smooth area of thermally treated samples, as determined by EDS.

Element (% weight)			Analysis site (see Fig. 4b)
Zn	Al	Cu	Point 1
76.23	22.32	1.45	

The thermally treated samples show a wide and smooth surface enclosing several small islands of light and dark shades, when observed under an optical or scanning elec-tron microscope at low magnifications (Figs. 4a and 4b). However, this surface is actually a substructure of two very fine, alternating constituents, one with a clear shade and the other with a dark shade, which are observable only at high magnifications under a scanning electron microscope (Figs. 4c and 4d).

The EDS findings of point 1 in Fig. 4b are presented in Table IV.

3.2. Compression tests

The compression curves constructed for the three sample sizes and for the as-cast and fine matrix microstructures of the borosilicate spheres - Zn22Al2Cu composites are shown in Fig. 5.

In general, three zones are identified in compression curves: in the first region, the elastic zone, stress varies linearly with strain until a maximum value of stress or collapse, followed by a decrease in stress; in the second region, stress stabilises at a specific value, defining a plateau; and in the third region, stress gradually increases with strain.
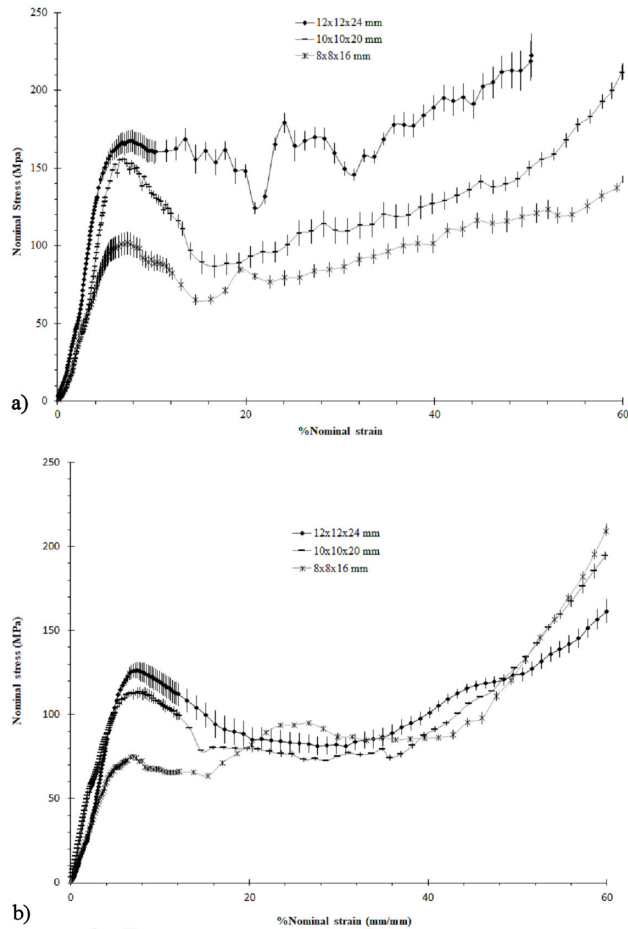
FIGURE 5. Compression curves of the borosilicate spheres - Zn22Al2Cu composite samples for the three sizes tested with a) as-cast and b) fine matrix microstructures.

In Table V are the Elastic modulus and Collapse stress values extracted from the stress-strain compression curves for each size and microstructure of the matrix. These parameters were defined and obtained from compression curves as was made in a previous work [22].

4. Discussion

4.1. As-cast microstructure

The as-cast microstructure, observed under an optical microscope, is in general similar to that observed under scanning electron microscope, with characteristic features of this type of structure.

The compositional analysis by EDS shows that the dendrites (Table III) feature a eutectoid composition, modified with Cu, and that the inter-dendritic regions feature an approximately eutectic composition of 94.5%p Zn and Al of the binary alloy system Al-Zn [23].

4.2. Thermally induced microstructure

This microstructure presents very fine constituents, with a mean size from 200 to 300 nm (Fig. 4d). The composition of a set of these fine grains is similar to that of the Zn-22Al eutectoid alloy, modified with Cu (Table IV).

4.3. Compression tests

The shape and number of regions of the compression curves are approximately similar to those of common foam metals [24]. However, the first maximum stress or collapse stress values of the latter, for example, are 9 to 17 times lower than the values assessed in this study, thus showing that the studied material features the dual nature of composite - foam. This result corroborates the findings reported by [22].

In the case of the as-cast matrix microstructure, the increase in size or number of embedded glass spheres gradually increases the level of the compression curve of composite (Fig. 5a). Namely, the composite supports a higher compressive stress: the elastic modulus, the value of collapse stress, the value after which stress decreases, the central value of stress defining the plateau and the level of the final region of the curve, known as densifica-tion region for foams and cellular materials, increase.

The as-cast matrix microstructure of the tested composites with the two smallest sizes experiences a small plastic deformation under a nearly constant stress, defining a plateau with slight stress changes in their stress-strain curves, and readily initiates the their densification, at strain values that slightly increase with composite size (lower section of Fig. 5a).

TABLE V. Elastic modulus and collapse stress obtained for each matrix microstructure and sample size.

	As-cast microstructure		Fine microstructure	
Sample size (mm)	Elastic Modulus (GPa)	Collapse Stress (MPa)	Elastic modulus (GPa)	Collapse stress (MPa)
$8 \times 8 \times 16$	19.05 ± 1.23	101.84 ± 7.24	17.16 ± 0.08	97.55 ± 0.21
$10 \times 10 \times 20$	27.58 ± 0.18	155.51 ± 1.47	20.22 ± 0.32	112.92 ± 3.16
$12 \times 12 \times 24$	33.07 ± 0.90	167.33 ± 7.08	22.05 ± 0.51	126.37 ± 4.80

In turn, the larger composite becomes permanently deformed to a greater extension at stresses with clearly marked ups and downs. Therefore, their densification starts at a higher strain, and the full shape of the resulting stress-strain curve, in the upper section of Fig. 5a, resembles the compression curves of cellular composites, such as Zn [25] and Al_2O_3 [26].

The above is undoubtedly caused by the increase in the number of spheres embedded in the matrix when increasing the composite size, and by the deformation macroscopic mechanism on compression of this composite with as-cast microstructure: this material is sequentially deformed in layers. That is, the matrix is plastically deformed until the stress on the spheres increases to a value that fractures them in an extreme layer of sample; decreasing then the total stress required, which after tends to increase during the closing and pressing of walls of holes in such layer, and thus, concurrently for the following layers. This mechanism was found and reported by [22], using a series of images of a sample of this composite with aforementioned microstructure in matrix and compressed in stages of increasing deformation.

The last region of the compression curves, known as densification region when material in compression is a foam, of the composite with the as-cast matrix microstructure starts at a plastic deformation that increases with the size of the material (17.82%, 21.80% and 32% of strain when increasing the sample volume to 1024 mm³, 2000 mm³ and 3456 mm³, respectively).

Conversely, the response to compressive stress of the composite with a fine matrix microstructure is completely different from that of the composites with an as-cast matrix microstructure. Thus, the following occurs when the size of the composite or the number of spheres embedded in the alloy matrix with fine microstructure increases: only the elastic modulus and the maximum stress (or collapse) after which stress decreases, increase.

In addition, the stress plateau remains at approximately the same level. No marked difference in the extension of the plateau is noted; the percentage of deformation at which densification starts decreases with the increase in sample size (42.8%, 36.0% and 30% of strain at sample volumes of 1024 mm³, 2000 mm³ and 3456 mm³, respectively), in contrast to the findings of the as-cast microstructure.

The behaviour of the composite with fine matrix microstructure would can be explained by the deformation macroscopic mechanism stablished and published by [22]: it was used a sample of this type of material and microstructure in matrix and was compressed in stages of increasing deformation. The spheres in sample broke simultaneously because the applied stress is directly transferred to spheres, due fine grains in alloy matrix do not deform because they have not dislocations [1].

Hence, the simultaneous rupture of all sample spheres cause the marked decrease in stress after reaching the collapse stress, and after this point, the composite behaves as a true foam, maintaining the plateau stress at a similar level, regardless of the composite size.

The pieces of spheres present in the samples with a fine matrix microstructure clearly prevent the deformation after constant or plateau stress; therefore, the closing and pressing of walls of holes in all sample start at increasingly lower deformations when the sample size increases or the number of pieces of spheres in matrix holes.

Figure 6 shows how the elastic modulus and the first stress maximum or collapse stress, in Table V, vary with the increases in sample volume of the tested composites. Both parameters clearly increase with the composite volume, regardless of the matrix microstructure: the elastic modulus and collapse stress continually increase in both types of microstructure. Whereas, the variation in first stress maximum is nearly asymptotic in the last two volume values of composites with the as-cast matrix microstructure.

The as-cast microstructure produces larger increases in elastic modulus and collapse stress than those generated by the fine microstructure when increasing the sample volume. Whereas the elastic modulus and collapse stress increase at a lower rate in the case of the fine microstructure.
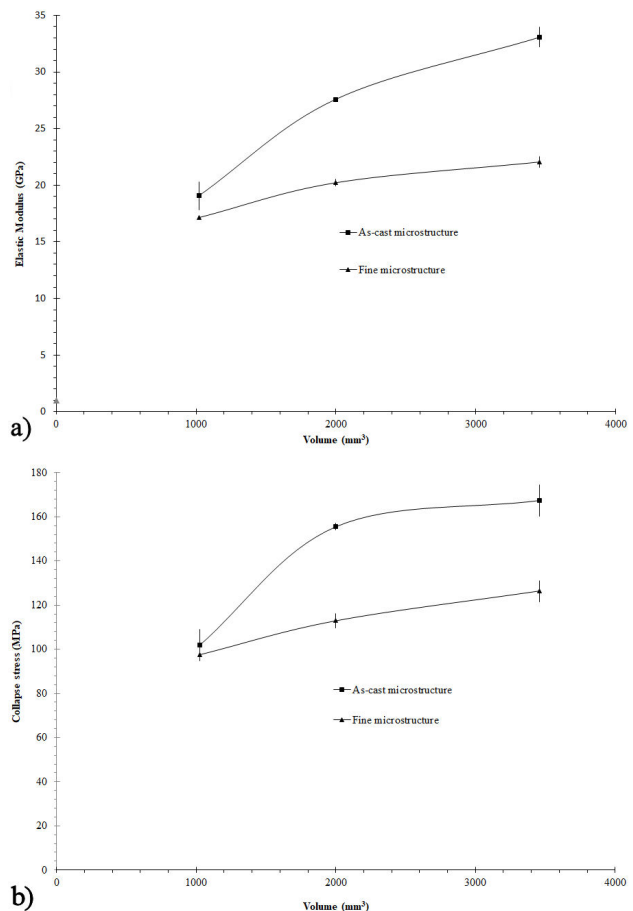
FIGURE 6. Variation of the a) elastic modulus and b) maximum stress or collapse in the compression test with increasing sample volume of each matrix microstructure of the borosilicate spheres - Zn22Al2Cu composites.

5. Conclusions

The compression behaviour of the studied composites is characterised by $\sigma - \varepsilon$ curves similar to those of foam or cellular metals. The composites with as-cast and fine microstructure in matrix have compression curves whose shape is similar to that exhibits by compression curves of ideal cellular metals, or cellular materials of Zn or Al_2O_3, respectively. The following occurs when increasing the composite size from a volume of 1024 mm^3 to 3456 mm^3, a) The level of the compression curve increases, the stress plateau goes from being almost imperceptible to having a greater extension, with marked stress fluctuations, and densification begins at higher values of plastic defor-mation, in the case of the as-cast matrix microstructure. b) The level of the first part of the compression curve (expressing the elastic behaviour and the collapse stress) increases, while the level of the stress plateau remains virtually un-changed, and densification begins at increasingly lower values of plastic deformation, in the case of the fine ma-trix microstructure. c) The as-cast microstructure produc-es greater increases in Young's modulus and collapse stress than those generated by the fine microstructure. Thus, the elastic modulus increases from 19 ± 1.23 GPa to 33.07 ± 0.9 GPa, and the collapse stress increases from 101.84 ± 7.24 MPa to 167.33 ± 7.08 MPa, in the case of the as-cast matrix microstructure. Whereas the elastic modulus and collapse stress increase at a lower rate, from 17.16 ± 0.08 GPa to 22.05 ± 0.51 GPa and from 97.55 ± 0.21 MPa to 126.37 ± 4.80 MPa, respectively, in the case of the fine matrix microstructure.

In general, borosilicate spheres - Zn22Al2Cu compo-sites show a foam compression mechanical behaviour that changes with the increase in size, and this change depends on the matrix microstructure: the as-cast microstructure is more susceptible to such a change than is the fine microstructure.

Acknowledgments

1. J.A. Aragon-Lezama, A. Garcia-Borquez and G. Torres-Villaseñor, *Mater. Sci. Eng. A.* **638** (2015) 165. doi: 10.1016/j.msea.2015.04.048

2. J.A. Aragón, J.R. Miranda, *Rev. Mex. Fis.* **51** (2005) 356. ISSN 0035-001X.

3. H.P. Degischer and B. Kriszt, *Handbook of cellular metals: Production, processing and applications*, (Wiley-VCH, Hoboken, New Jersey 2002), pp. 188. doi:10.1002/3527600558.

4. A. Daoud, *Mater. Sci. Eng. A* **488** (2008) 281-295. doi:10.1016/j.msea.2007.11.02.

5. A. Daoud, *Mater. Sci. Eng. A* **525** (2009) 7-17. doi: 10.1016/j.msea.2009.05.038.

6. S. Diel *et al.*, *J Mater Sci* **47** (2012) 5635-5645. doi: 10.1007/s10853-012-6432-0.

7. L.J. Gibson, *Ann. Rev. Mater. Sci.* **30** (2000) 191-227. doi:10.1146/annurev.matsci.30.1.191.

8. G.M. Gladysz, K.K. Chawla, A.R. Boccaccini, *J Mater Sci* **47** (2012) 5625-5626; doi: 10.1007/s10853-012-6503-2.

9. C. Kádár *et al.*, *Mater.* **10** (2017) 196-205. doi:10.3390/ma10020196.

10. B. Katona1, I.N. Orbulov, *Period. Polytech. Mech. Eng.* **61** (2017) 146-152. doi: 10.3311/PPme.103456.

11. B. Katona, G. Szebényi, I. N. Orbulov, *Mater. Sci. Eng. A* **679** (2017) 350-357. doi: 10.1016/j.msea.2016.10.061.

12. D. Lehmhus *et al.*, *Procedia Mater. Sci.* **4** (2014) 383-387. doi: 10.1016/j.mspro.2014.07.578.

13. F.W. Ling, D.E. Laughlin, *Metall. Trans A* **10** (1979) 921-928. doi:10.1007/bf02658311.

14. K. Májlinger and I.N. Orbulov, *Mater. Sci. Eng. A.* **606** (2014) 248-256; doi: 10.1016/j.msea.2014.03.100.

15. E. Martinez-Flores, G. Torres-Villaseñor, *Hibrid materials based on Zn-Al alloys*, in: J. Cuppoletti (Ed.), Metal, Ceramic and Polymeric Composites for Various Uses (InTech, Florida, US, 2011), pp. 149-170. (Chapter 7). doi: 10.5772/17241.

16. I.N. Orbulov and J. Ginsztl, *Compos. A* **43** (2012) 553-561. doi: 10.1016/j.compositesa.2012.01.008.

17. I.N. Orbulov and A. Szlancsik, *Adv. Eng. Mater.* **20** (2018) 1-12. doi: 10.1002/adem.201700980.

18. L. Pan *et al.*, *Mater. Sci. Eng. A* **731** (2018) 413-422. doi: 10.1016/j.msea.2018.06.072.

19. A.A. Presnyakov, Y.A. Gorban, V.V. Chernyakova, *Russ. J. Phys. Chem.* **35** (1961) 623-633.

20. A. Sandoval-Jimenez, J. Negrete, G. Torres-Villaseñor, *Mater. Charact.* **61** (2010) 1286-1289. doi:10.1016/j.matchar.2017.07.014.

21. A. Szlancsik *et al.*, *Mater. Des.* **83** (2015) 230-237. doi: 10.1016/j.matdes.2015.06.011.

22. A. Szlancsik *et al.*, *Mater.* **8** (2015) 7926-7937. doi: 10.3390/ma8115432

23. H. Thornton and C. L. Magee, *Metall. Trans.* **6A** (1975) 1801. doi: 10.1007/BF02658535.

24. G. Torres, J. Negrete, L. Valdés, *Rev. Mex. Fis.* **31** (1985) 490. ISSN 0035-001X.

25. J. Weise *et al.*, *Adv. Eng. Mater.* **15** (2013) 118-122, doi: 10.1002/adem.201200129.

26. Y.Y. Zhao and X.F. Tao, *Mater. Sci. Technol.* (2009) 1785-1794.